ECS Transactions, 63 (1) 137-144 (2014)
10.1149/06301.0137ecst ©The Electrochemical Society

Electrochemical Properties of $CeVO_4$ and $FeVO_4$ at High Temperatures

Timea Behofsits[a], Georg Pani[a], Markus Gross[a], Günter Fafilek[a] and Marcin Malys[b]

[a] Institute of Chemical Technologies and Analytics,
Vienna University of Technology, A-1060 Vienna, Austria
[b] Faculty of Physics, Warsaw University of Technology, PL-00-662 Warszawa, Poland

High temperature corrosion of steel is dramatically accelerated by ashes and scales containing compounds of iron, vanadium, oxygen and sulfur. High temperature electrochemical impedance spectroscopy (HT-EIS) and cyclic voltammetry (HT-CV) on ash samples from a heavy crude oil furnace, showed high conductivity of at least one of the several existing phases and also some redox activity, which could be related to redox processes of vanadium containing compounds. On the one hand, it is unfavorable for the corrosion stability of construction materials; on the other hand it might be an effective material for several applications, like high temperature fuel cells electrodes, intercalation materials in ion-batteries or as catalyst.
$FeVO_4$ was identified as one of the few potentially highly conductive phases in the ash. Pure $FeVO_4$ was synthesized and investigated by HT-EIS and HT-CV on micro-samples. For comparison $CeVO_4$ was included in this investigation.

Introduction

Sulfur and sodium create molten phases on the surface of steel accelerating oxidation at high temperatures known as “hot corrosion” (1). Vanadium or other elements like molybdenum or boron additionally form phases with low melting point and further increase corrosion rate. Investigation of the electrical properties of ash samples revealed a high electrical conductivity. From impedance data it was concluded that the electrical conductivity is mainly electronic. In addition, redox reactions were observed in vanadium containing ash samples by high temperature voltammetry (2). By comparison of the measured redox potential with the value calculated from Gibb’s enthalpy of formation (2, 3) this was associated with the reaction

$$V^{5+} + e^- \rightleftarrows V^{4+} \qquad [1]$$

The high conductivity and the apparent high reactivity for the oxygen reduction reaction draw our interest to the phase which is responsible for the electrical and electrochemical properties of the ash. It turned out that $FeVO_4$ is one of the main constituents of the ash which has interesting properties and applications like as selective catalyst, gas sensor or electrodes in lithium batteries (4 - 7). Therefore, pure $FeVO_4$ was synthesized and investigated by HT-EIS and HT-CV on micro-samples.

For comparison $CeVO_4$ was included in this investigation. $CeVO_4$ and its derivatives, due to unique optical, electrical (high electrical conductivity as a p-type semiconductor)

and redox properties, have been viewed as prospective materials for microelectronic applications as a counter electrode in electro-chromic windows, luminescent materials, gas sensors, oxidation catalysts and components of solid oxide fuel cell (SOFC) anodes (8 - 13).

Experimental

Sample preparation

$FeVO_4$ and $CeVO_4$ materials were prepared by the solid state route from the oxides. Oxides with purity of 99.99% or better were purchased from Aldrich. Oxides were mixed together in the proper molar ratio and ground in the mortar. After calcination for 24 hours at 600 °C and 50 hours at 800 °C for $FeVO_4$ and $CeVO_4$ respectively, the material was ground and calcined again. Phase purity was checked by XRD.

The material for impedance spectroscopy samples was ground very carefully together with ethanol and camphor as a pressing aid to get a fine and homogeneously grained powder. The powder was pressed to pellets in an iso-static press. Pellets with a diameter of 10 mm and varying thickness of approximately 3-5 mm were obtained and sintered at 800 °C for 2 hours in case of $FeVO_4$ and at 950 °C for 22 hours in case of $CeVO_4$.

Platinum electrodes were applied by painting platinum paste on both large opposing areas on $FeVO_4$ pellets. Silver paste electrodes were used in case of $CeVO_4$. Samples with the electrodes were fired before mounting them into the sample holder for impedance spectroscopy.

For the voltammetric experiment, small grains of the phase pure material were used; therefore no further treatment was necessary.

Measurements

Impedance spectra were measured in a 2-probe setup. Contacts to the electrodes were made with two platinum plates connected to separate shielded leads for current and voltage for the signal High and Low. The holder is designed for measurements from room temperature up to 800°C. The set-up, consisting of a Solartron 1260 impedance meter and a furnace with double loop temperature control, was operated by in-house developed software. Spectra were measured between 0.1 Hz and 1 MHz with a signal level of 50mVpp.

The voltammetry was done in a cell with yttria stabilized ziconia (YSZ) as an oxygen ion conducting support for counter electrode, reference electrode and the sample as a working electrode. The samples are very small grains which are placed on top of the YSZ and contacted with a platinum plate. A schematic drawing is shown in fig. 1. The cell is positioned inside a similar holder like for the impedance measurement. The whole cell can be flushed with inert gas. Naturally, there is still some residual low but unknown oxygen partial pressure inside. Consequently, the potential of the reference electrode is unknown. Therefore, a measurement is made on copper for calibration of the reference potential before and after the measurement on the sample. A detailed description of the method is given in (3, 14). Voltammograms were measured at a scan rate of 10 mVs^{-1} in a wide potential range between -1.5 V and +0.3 V versus the reference electrode. Potential scale was corrected with respect to the potential of the reversible oxygen electrode at standard-pressure $pO_2 = 10^5$ Pa (ROE) at the particular temperature.

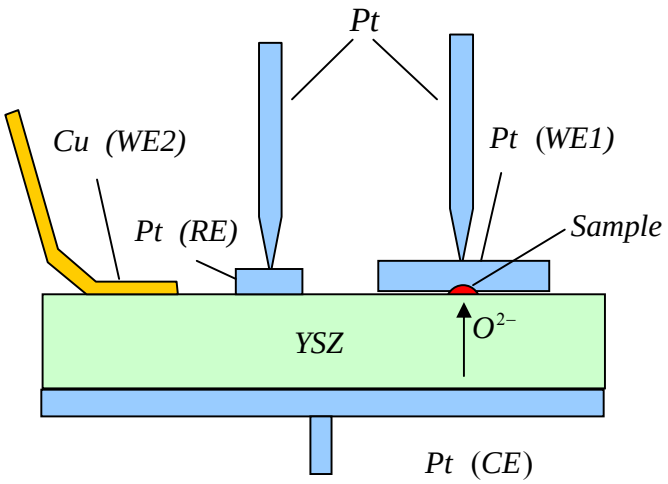

Figure 1. Schematic drawing of the cross-section of the electrochemical cell.

Results and Discussion

Impedance spectroscopy and electrical conductivity

Impedance spectra for $FeVO_4$ are shown in fig. 2 for the lower temperatures. The single arc observed in the complex plane impedance plot indicates predominant electronic conductivity of the bulk. The Ohmic resistance of the sample was obtained by extrapolating the semicircle to the real axis at low frequencies. Conductivity was calculated from the resistance value and the geometric factor of the pellet. The temperature dependence of the conductivity follows the Arrhenius relationship.

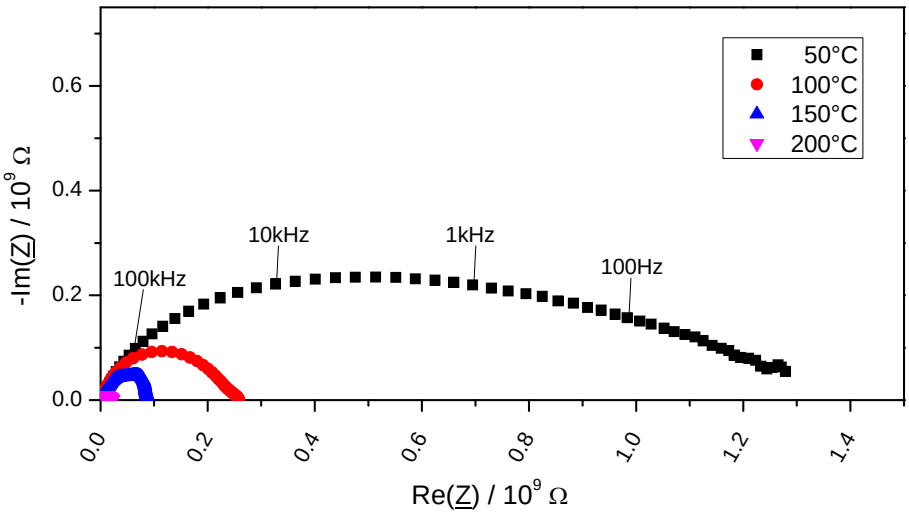

Figure 2. Complex plane plot of the impedance for $FeVO_4$.

Two linear regions are observed in the Arrhenius plot in fig. 3 with the transition at about 577°C. This might be either related to a phase transition, ordering/disordering phenomena or the transfer from one to another conduction mechanism. The formation of a melt can be excluded because the melting temperature of $FeVO_4$ lies above 850°C. This phenomenon is not in the focus of this work; therefore it will not be discussed in detail. The comparison with the electrical measurements on the ash samples show some analogy with respect to the shape of the impedance spectra, the two linear regions in the Arrhenius plot and the transition temperature. Therefore, it seems that indeed the iron-vanadate dominates the electrical properties of the ash.

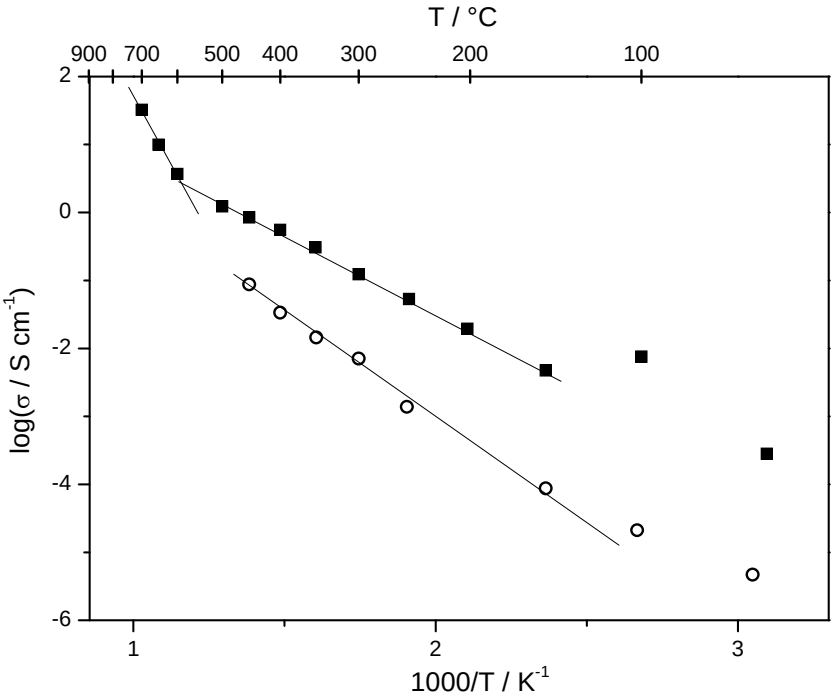

Figure 3. Arrhenius plot of the conductivity for $FeVO_4$ (solid rectangles) and $CeVO_4$ (open circles).

The impedance spectra for $CeVO_4$ are displayed in fig. 4. In contrast to, a second arc is observed at low frequencies. This might be related to an electrode process, concluded from the relatively large time constant. It indicates that the transference number for the electronic charge carriers is not unity. The temperature range for the measurement was restricted to a maximum of 450°C because of the silver electrodes. Silver easily reacts with the material and forms $AgVO_4$ as it was found for $FeVO_4$ (15). In our measurements, a similar behavior was observed for $CeVO_4$.

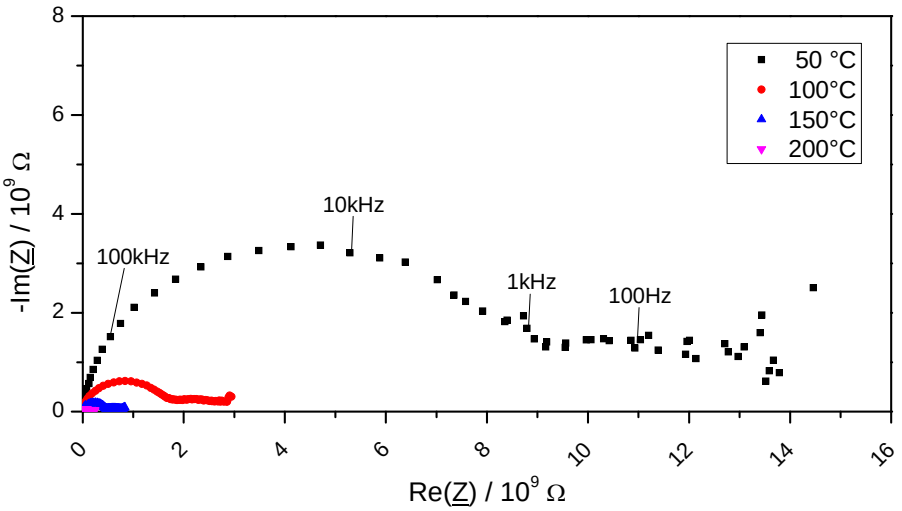

Figure 4. Complex plane plot of the impedance for $CeVO_4$.

Figure 3 displays the Arrhenius-plot for the conductivity of $CeVO_4$. Within the investigated temperature range no change of the slope was observed. At 450 °C, the conductivity is about one order of magnitude lower than for the $FeVO_4$.

Cyclic voltammetry

The voltammogram of a $FeVO_4$ microsample taken at 600 °C is shown in fig.5. A redox process is observed at a potential of about -0.35 V vs. the reversible oxygen electrode at 10^5 Pa. This value fits to the thermodynamic value of -0.3 V at this temperature of the redox reaction of vanadium given by equation [1].

Since in $FeVO_4$ iron is in the 3+ valence state the influence of the redox reaction [2] cannot be excluded.

$$2Fe^{3+} + e^- \rightleftarrows Fe^{3+}Fe^{2+} \qquad [2]$$

In the pure iron/ iron-oxide system, Fe^{3+} is reduced to the 2+/3+ state according to reaction [3].

$$2Fe_2O_3 \rightleftarrows 3Fe_3O_4 + \tfrac{1}{2}O_2 \qquad [3]$$

The calculated potential value for the related redox reaction [2] is about -0.61 V at 600 °C. Even if the potential values do not agree very well, this reaction might be responsible for the observed redox process because the calculation is done for the iron oxide and overall reaction [3] and not for the iron vanadate.

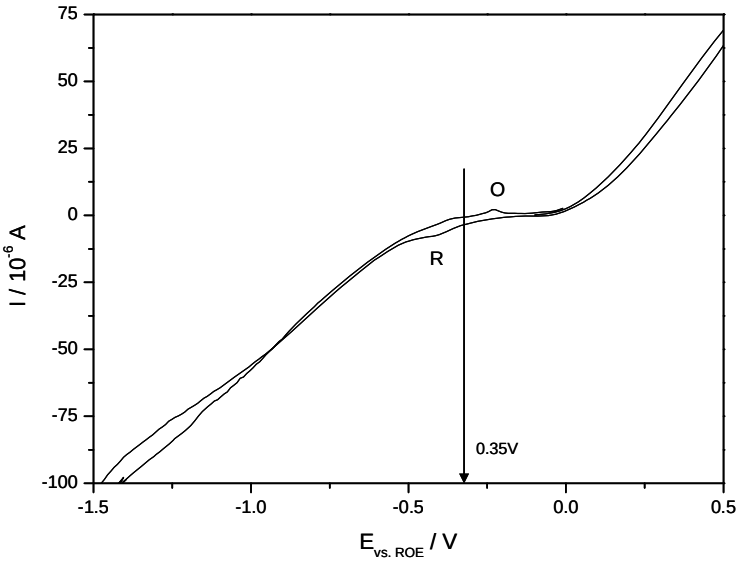

Figure 5. Voltammogram on $FeVO_4$ taken at 600 °C.

On the other hand, the voltammogram on cerium vanadate in fig. 6 shows current peaks of a redox reaction in a similar potential range as well. Iron cannot be responsible for the oxidation/reduction peaks found at approximately -0.45 V, naturally.

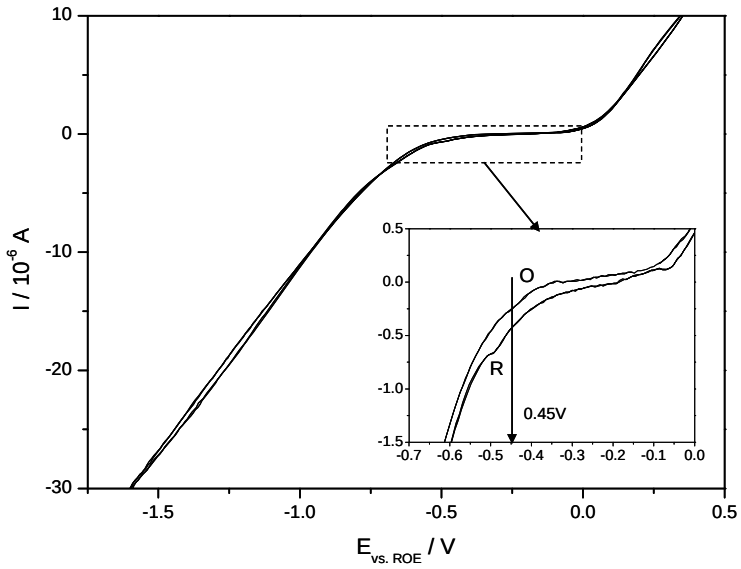

Figure 6. Voltammogram on $CeVO_4$ taken at 600°C.

From the overall shape of the voltammograms, the stability of the material seems to be high. No additional reduction peak or significant hysteresis between the cathodic and the anodic scan was observed until about -1.5 V. The relatively large reduction current at large negative polarization indicates fast kinetics for the oxygen reduction reaction of the residual oxygen inside the chamber. Considering the linear relationship between applied

potential and current, the current is mainly limited by the Ohmic resistance of the YSZ. At positive potentials the oxygen evolution reaction takes place. It shows also a high reaction rate, again limited by the Ohmic resistance of the cell.

A comparison between redox potentials evaluated from the oxygen partial pressure stability limit of $CeVO_4$ for the reaction

$$CeVO_4 \rightleftarrows CeVO_3 + \tfrac{1}{2} O_2 \qquad [4]$$

calculated by Danilovic et.al. (16) with the measured redox potentials at 600 °C (fig. 7) reveals that the values lie lower than the stability limit of $CeVO_4$.

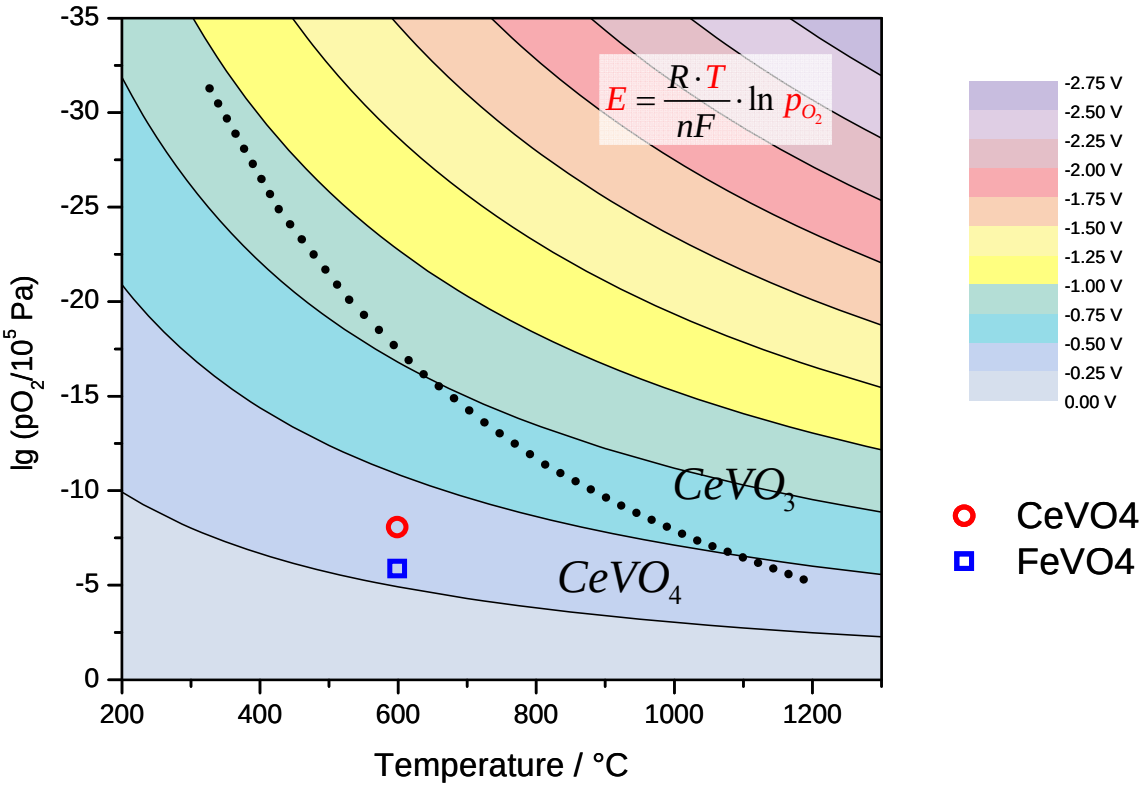

Figure 7. Comparison of measured redox potential (symbols) with calculated stability of $CeVO_4$ against reduction (dotted line). Contour plot shows the relationship between $lg(pO_2)$ and potential of a reversible oxygen electrode vs. the reference value at 10^5 Pa as a function of temperature.

Conclusions

Redox processes were observed in $CeVO_4$ below the calculated stability border for $CeVO_4$. Similar redox processes were found for $FeVO_4$. This could be related to changes of oxygen stoichiometry in the material and the accompanied reduction/oxidation of vanadium ($V^{5+} \leftrightarrow V^{4+}$).

Acknowledgments

The support of this work by the Austrian funding agency OeAD-GmbH within the wtz-program, project PL04_2012, is gratefully acknowledged.

References

1. R. Bürgel, H.J. Maier, T. Niendorf, in *Handbuch Hochtemperatur–Werkstofftechnik*, Springer Fachmedien Wiesbaden GmbH (2011).
2. G. Pani, Diploma theses, TU-Vienna (2013).
3. G. Fafilek, S. Harasek, *Solid State Ionics*, **119,** 91 (1999).
4. P.I. Cowin, R. Lan, L. Zhang, C.T.G. Petit, A. Kraft, S. Tao, *Mater. Chem. Phys.*, **126,** 614 (2011).
5. G. Mangamma, E. Prabhu, T. Gnanasekaran, *Bull. Electrochem.*, **11–12**, 696 (1996).
6. P. Poizot, E. Baudrin, S. Laruelle, L. Dupont, M.Touboul, J.M. Tarascon, *Solid State Ionics*, **138**, 31 (2000).
7. S. Denis, E. Baudrin, F. Orsini, G. Ouvrard, M. Touboul, J.M. Tarascon, *J. Power Sources*, **81**, 79 (1999).
8. G. Picardi, F. Varsano, F. Decker, A. Surca, B. Orel, *Electrochim. Acta*, **44**, 3157 (1999).
9. A.M. Salvi, F. Decker, F. Varsano, G. Speranza, *Surf. Interface Anal.*, **31**, 255 (2001).
10. S. Varma, B.N. Wani, N.M. Gupta, *Mater. Res. Bull.*, **37**, 2117 (2002).
11. A. Watanabe, *J. Solid State Chem.*, **153**, 174 (2000).
12. V.V. Kharton, A.A. Yaremchenko, A.A. Valente, V.A. Sobyanin, V.D. Belyaev, G.L. Semin, S.A. Veniaminov, E.V. Tsipis, A.L. Shaula, J.R. Frade, J. Rocha, *Solid State Ionics*, **176**, 781 (2005).
13. E. V Tsipis, V. V Kharton, J.R. Frade, *J. Eur. Ceram. Soc.*, **25**, 2623 (2005).
14. G. Fafilek, *Solid State Ionics*, **113-115,** 623 (1998).
15. P.I. Cowin, R. Lan, L. Zhang, C.T.G. Petit, A. Kraft, S. Tao, *Materials Chemistry and Physics*, **126(3)**, 614 (2011).
16. N. Danilovic, J.L. Luo, K.T. Chuang, A.R. Sanger, *Journal of Power Sources*, **192**, 247 (2009).